SERI/TP-253-2794
UC Category: 64
DE85012176

System Studies of Open-Cycle OTEC Components

Brian K. Parsons
Harold F. Link

September 1985

Prepared for Ocean '85
San Diego, California
12-14 November 1985

Prepared under Task No. 4006.31
FTP No. 523

Solar Energy Research Institute
A Division of Midwest Research Institute

1617 Cole Boulevard
Golden, Colorado 80401-3393

Prepared for the
U.S. Department of Energy
Contract No. DE-AC02-83CH10093

Printed in the United States of America
Available from:
National Technical Information Service
U.S. Department of Commerce
5285 Port Royal Road
Springfield, VA 22161

Price: Microfiche A01
Printed Copy A02

Codes are used for pricing all publications. The code is determined by the number of pages in the publication. Information pertaining to the pricing codes can be found in the current issue of the following publications, which are generally available in most libraries: *Energy Research Abstracts, (ERA); Government Reports Announcements* and Index (*GRA* and I); *Scientific and Technical Abstract Reports (STAR);* and publication, NTIS-PR-360 available from NTIS at the above address.

SYSTEM STUDIES OF OPEN-CYCLE OTEC COMPONENTS

Brian K. Parsons
Harold F. Link

Solar Energy Research Institute
1617 Cole Boulevard
Golden, Colorado 80401

ABSTRACT

A system model of open Rankine cycle ocean thermal energy conversion (OC-OTEC) was used to examine the effects of component performance and design on plant cost. Three components are examined in detail: an optional seawater deaeration subsystem, the flash evaporator, and a two-stage direct-contact condenser. Preliminary data quantifying noncondensable gas release in upcomers and a de-bubbler chamber were used to evaluate the effect of predeaeration (removing the dissolved gases in deaeration chambers before the seawater enters the heat exchangers) on system cost and performance. Little data on the interactions between geometry and performance of vertical spout flash evaporators operating under OTEC conditions are available; therefore, we performed independent parametric variations. For the direct-contact condenser previous numerical studies provide the basis for coupling geometry and performance. Results of these studies are useful in setting research priorities, in defining operating conditions for further seawater experiments, and in updating plant cost estimates.

1.0 INTRODUCTION

1.1 Resource and Technology

The oceans contain a great amount of stored thermal energy. The temperature difference between the surface and deep water creates thermal gradients that can be turned into electricity. The conversion technology is similar to that used in conventional power plants. The sensible energy contained in the warm surface water is used to vaporize a working fluid that is then expanded through a turbine connected to an electric generator. A condenser maintains low pressure at the turbine exit using cold seawater as the energy sink.

Over a century ago, d'Arsonval[1] first suggested using ocean thermal gradients to generate power using a closed-cycle system. This system uses a secondary working fluid, such as ammonia, to drive a turbine. Surface heat exchangers evaporate and condense the working fluid while separating the working fluid from the seawater. Using a secondary working fluid allows the power cycle to operate at a higher pressure.

In 1930, George Claude,[2] a student of d'Arsonval, proposed and demonstrated an alternative cycle, the open cycle, that uses steam evaporated directly from the seawater to power a turbine. Since the seawater temperature is less than the normal boiling point at atmospheric pressure, the power cycle pressure must be subatmospheric. Low pressure at the turbine exit may be maintained by a surface condenser, which has an added benefit of producing fresh water as a by-product, or by a direct-contact condenser in which the steam condenses directly on the cold seawater.

In 1979, Westinghouse Electric Corporation completed a comprehensive analysis of a 100-MW_e net floating, open cycle plant for the Department of Energy.[3] The analysis projected that floating plants in the range of 35-100 MW_e would be cost-effective. The report identified several technical uncertainties and unknowns along with their potential for improving the plant's performance and economic viability. The largest potential cost impacts were associated with the evaporator, mist removal device, and condenser. Since that time, research at the Solar Energy Research Institute (SERI) and its contractors has addressed these and other important issues.[4-26]

1.2 Open-Cycle System Description

A block diagram of the basic open-cycle system is presented in Fig. 1. Warm tropical seawater (~25°C) is pumped from near the ocean surface into an evacuated evaporator chamber where the pressure is lower than the corresponding saturation condition of the entering seawater. Flash evaporation results, cooling the seawater and converting a small portion of it (0.5%) to low-pressure steam.

The cooler seawater (~20°C) is then discharged back into the ocean. For some evaporator designs, the boiling process may entrain seawater in the steam, causing corrosion and erosion of the turbine blades. To mitigate this problem, a mist removal device may be required.

The steam expands through a turbine and a diffuser towards the condenser. A generator connected to

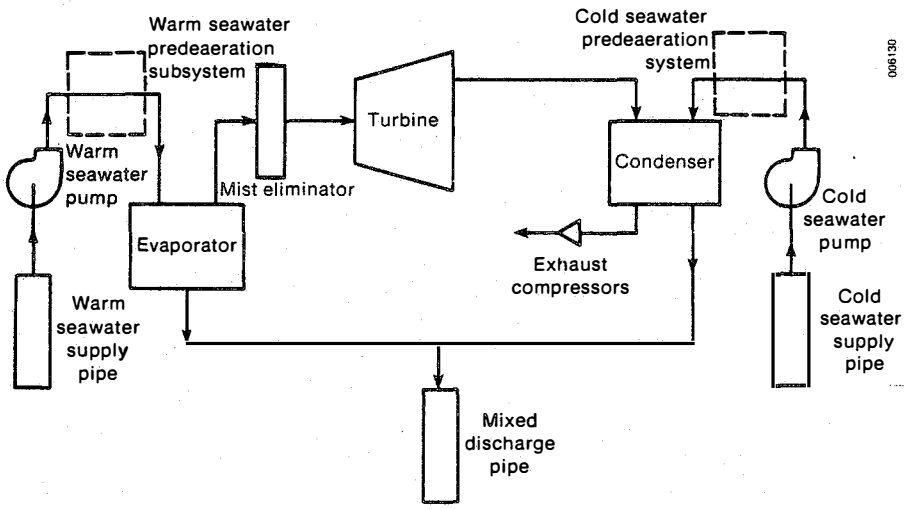

FIG. 1 OPEN RANKINE CYCLE OTEC SYSTEM

the turbine produces the electric power, which also operates the seawater pumps and the exhaust compressors.

Cold seawater (~5°C) is pumped from depths of around 1000 m into the condenser to maintain the condenser pressure. Dissolved gases, present in the seawater, may come out of solution. To prevent an increase in pressure and loss in efficiency in the condenser, these gases, along with air leakage into the vacuum enclosure, must be removed by an exhaust system.

Some of the dissolved noncondensable gases may be removed from the warm and cold seawater before entering the main power system. These optional seawater predeaeration components operate at pressures greater than the seawater vapor pressure but low enough to allow noncondensable gas desorption.

1.3 Current Status

Recent studies have shown that small-scale, land-based plants can be economic in the short term. The longer seawater supply pipes required by land-based facilities increase parasitic pumping power and capital cost but eliminate the technical risk and uncertainty associated with mooring or station keeping of large floating structures, delivery of energy to shore, and the effects of plant motion on the power cycle.

Smaller capacity plants (on the order of 10-50 MW_e) are expected to penetrate the high energy cost island market in a much shorter time than large-capacity plants. In addition, many of these island communities are in need of increased freshwater supplies. If a surface condenser (i.e., shell and tube or plate-fin) is used, an OC-OTEC system produces a significant amount of fresh water, nearly 200 kg/s (4 million gal/day) for a 10-MW_e plant. Another factor is that the perceived investment risk for a first generation OC-OTEC plant is high. By concentrating research on a smaller plant, which would require a much lower total capital investment, the difficulty of financing is lessened. Our research has shown preliminary costs of around $7200/kW for a typical 10-MW_e-capacity plant.

The technical feasibility of OC-OTEC was established when Georges Claude demonstrated the principles in an operating plant in the 1930s. Numerous studies have addressed the simultaneous heat and mass transfer processes in the direct-contact heat exchangers both analytically and experimentally.[4,5,7-9,12,17-22] These studies have considerably increased our understanding of the candidate geometries for the evaporator and direct-contact condenser. A major limitation at this time is that most experiments have used fresh water. Performance with seawater might be significantly different, and only limited experiments with seawater have been performed.[20] The effects of the presence of nucleation sites as well as other differences between fresh water and seawater, such as surface tension, natural surfactants, and boiling point elevation, are not well understood.

Performance and life expectancy of the low-pressure turbine is an area of continuing investigation. In their 1979 study and in a follow-up study, Westinghouse[3,24] identified the potential for manufacturing very large (45-m) turbines corresponding to a gross power of 140 MW_e. The blade manufacturing concept used composite manufacturing techniques similar to helicopter rotor technology. More recently, smaller scale metal blade (1-3 MW_e) concepts have been presented using conventional low-pressure stage rotors and slightly modified stators.[25,26] We believe a turbine of this type could be designed with very little development work. The largest remaining turbine unknown is the amount and the magnitude of the effects of seawater droplets entrained in the steam (which could cause erosion and corrosion of the

blades). Another issue is off-design point performance and the best control strategy to maintain maximum output.

Seawater pumps and exhaust compressors are available as off-the-shelf items, and little research has addressed these components. Corrosion and maintenance in the seawater environment is a problem, but these issues are not critical and are being examined by manufacturers for many applications.

For 5-10 MW_e capacity plants the technology exists for manufacturing conventional seawater supply pipes of sufficient diameter (2-4 m). However, the diameter dictated by larger plants would require manufacturing technology development. For relatively small rigid pipes the major remaining unknown is related to deployment. In addition, many issues remain regarding steep undersea slope stability, currents, storms, etc., and their effect on different pipe designs. Several advanced concepts such as undersea drilling and "inflatable" pipes with a submerged pump can greatly reduce cost to the level of the long-term DOE goal and are currently being examined. It is beyond the scope of this paper to thoroughly address research in this area, but several critical issues remain.

Currently, the Natural Energy Laboratory of Hawaii (NELH), located on the west coast of the island of Hawaii at Keahole Point, is investigating many of the research issues associated with OTEC[17,20] with funding from DOE, the state of Hawaii, and private companies. Other projects--for example, mariculture and seawater corrosion--are also being performed at NELH with both public and private funding. NELH is the only laboratory experimenting with actual seawater. Existing seawater supply pipes deliver around 32 kg/s (500 gal/min) of cold seawater at 8°C and 65 kg/s (1000 gal/min) of warm seawater at 26°C. Future plans include expanding the facility to accommodate critical component and integrated cycle experiments.

2.0 SYSTEM MODEL

2.1 General Description

The computer model of an open-cycle system consists of subroutines that simulate the components shown in Fig. 1. Besides these subroutines the model includes a subroutine that calculates the inter-component steam pressure losses. The component performance modeling equations are described by Parsons et al.[10,14] with the exception of the condenser model, which has been updated since these reports.[19] A brief description of the solution method is as follows: four temperatures are chosen at the onset, the warm water inlet, the evaporator steam outlet, the turbine outlet, and the cold water inlet. For a given warm water flow rate the warm water outlet temperature is found from the evaporator effectiveness (ε) defined as:

$$\varepsilon = (T_{wi} - T_{wo})/(T_{wi} - T_s) , \qquad (1)$$

where T_{wi} is the warm water inlet temperature, T_{wo} is the warm water outlet temperature, and T_s is the steam outlet temperature. In this paper we used an IR-100-award-winning vertical spout evaporator design[27] with a nominal effectiveness of 0.90. The steam mass flow rate is then found from a heat balance. We can find the noncondensable gas release from the warm seawater from inlet conditions and the input percentage of equilibrium achieved. Air leakage into the vacuum chamber is included as an input. Pressure (and corresponding temperature) drops in the mist eliminator[6] and steam passageways are found using input pressure drop coefficients ("K" factors). With the turbine inlet temperature, outlet temperature, steam mass flow rate, and a specified isentropic efficiency we can compute the turbine power output. By applying a generator efficiency we can find the gross electric power of the plant. A diffuser component converts some of the steam velocity head at the turbine exit into increased steam temperature and pressure using an input diffuser recovery factor. The condenser model calculates four quantities: percentage of steam condensed, percentage of dissolved inert gas release, steam outlet temperature, and vapor side pressure drop for the cocurrent and countercurrent sections from equations derived from the results presented in Bharathan et al.[19] The fitted curves of performance are functions of inlet conditions such as steam temperature, superheat, and noncondensable gas content in the steam plus condenser design conditions such as vapor loading, Jacob number, condenser height, and liquid-vapor interfacial area per unit volume. The cold seawater flow rate is found from the Jacob number, steam loading, and steam temperature. A vent compressor train with interstage coolers then exhausts the uncondensed steam and noncondensable gases to the atmosphere. The power required to run the compressors is subtracted from the gross generator output. In addition, head losses in the seawater supply and discharge pipes are found for specified pipe lengths and flow velocities. The model then finds the parasitic pumping power and the net electric output of the plant.

Component sizing is found from flow rates and loadings or velocities. Costs are computed as a function of size using Block et al.[13] and Valenzuela et al.[16] with small modifications, such as including a cost for condenser fill such as packing or plates associated with a falling film. We then estimate additional costs such as plant design and engineering, land, support buildings, controls, etc. The installed power cost in $/watt is simply the net electric output divided by the total cost. The interested reader may find the details of the system model and the coded equations in the earlier listed reference citations. For this study the nominal net installed power value was approximately 10 MW_e. The key input and reference parameters are listed in Table 1.

2.2 Optimization

The design parameters included in Table 1 correspond to typical OTEC conditions or standard

Table 1. Constant Plant Parameters

Component Parameter	Value
Warm seawater flow rate	34620 kg/s
Warm seawater inlet temperature	25°C
Cold seawater inlet temperature	5°C
Evaporator height	0.5 m
Evaporator passage K factor	0.5
Mist removal K factor	10.0
Turbine passage K factor	1.0
Turbine efficiency	0.8
Generator efficiency	0.9
Turbine hub-to-tip ratio	0.44
Diffuser efficiency	0.9
Cocurrent condenser type	falling film
Countercurrent condenser type	packed column
Combined compressor and motor efficiency	0.72
Intercooler pressure drop	150 Pa
Compressor pressure ratios	1.6
Combined pump/motor efficiency	0.78
Warm seawater supply pipe length	300 m
Cold seawater supply pipe length	2200 m
Mixed discharge pipe length	1100 m
Pipe cost	1200 $/m length m diameter

industrial component performance and design. These parameters were not varied during optimization studies. Other design parameters (Table 2) may be varied to obtain a minimum installed power cost design. For example, the temperature distribution between components is varied by changing the value of the evaporator steam temperature and the turbine outlet temperature. Another variable that was examined in the overall optimization was the steam velocity through the mist eliminator. Increasing velocity causes a larger pressure drop (which reduces the energy extracted by the turbine), but reduces the area and cost of the device. The other main variables examined in this paper are related to the heat exchanger design conditions.

Geometric design variables such as evaporator spout diameter, seawater velocity in the spouts, spacing between spouts, and spout height affect not only the evaporator cost but the structure cost (mainly because of vacuum containment size) and seawater pumping power as well. Varying these design parameters will most likely affect evaporator effectiveness, but the coupling between the above geometric variables and performance is not available. Therefore, we chose nominal conditions for each variable and did not include evaporator performance and geometry in the overall system optimization. Individual parametric variations and the nominal values of evaporator variables are discussed later.

Condenser design parameters affect the system installed power cost by changing the component cost, structure cost, cold seawater pumping power, the pipe design, and vent compressor parameters in a fashion similar to the evaporator design. In contrast to the evaporator, however, we use relations coupling the geometry and inlet conditions to the condenser performance. Therefore, overall system optimization includes condenser loadings and geometry as variables. The geometric variables included in optimization include gas loading (kg/s m^2), condenser height, liquid-vapor interfacial area per unit volume, and a modified Jacob number defined as:

$$Ja = m_w C_p (T_{wo} - T_{wi})/m_s h_{fg} , \qquad (2)$$

where m_w is the water flow rate, C_p is the specific heat of seawater, m_s is the steam flow rate, and h_{fg} is the enthalpy of vaporization. Changes in performance and required capital are reflected in the overall system installed power cost.

The final set of parameters included in this optimization determines the seawater supply pipe cost and head losses. For a predetermined water flow rate, the flow velocities of the seawater are varied to determine pipe diameter. Lower velocity decreases head loss and parasitic pumping power while increasing pipe costs. All these parameters are varied until the optimum lowest installed power cost plant is found.

A third category of parameters is also of concern. A large uncertainty exists in the structure costs associated with the vacuum containment vessel. A preliminary estimate was developed for a 10-MW_e, land-based plant of $10,000/$m^2$.[16] Depending on the portion of the structure costs that are independent of planform area and the relation between total planform area and heat exchanger area, the incremental change in structure cost for small changes in heat exchanger size could vary from around $5,000 to $25,000/$m^2$. Condenser and evaporator studies were performed at both of these values to access the effect of changing the structure cost penalty on optimum design conditions.

Table 2. Plant Parameters Varied in Optimization

Component	Parameter
Evaporator	Steam outlet temperature
Turbine	Steam outlet temperature
Warm seawater supply pipe	Seawater flow velocity
Cold seawater supply pipe	Seawater flow velocity
Mixed discharge pipe	Seawater flow velocity
Mist eliminator	Steam flow velocity
Cocurrent condenser	Height
	Gas loading
	Jacob number
	Surface area to volume ratio
Countercurrent condenser	Height
	Gas loading
	Jacob number
	Surface area to volume ratio
Seawater predeaeration subsystems	Number of stages

A similar situation exists with the seawater piping costs. Pipe costs have been estimated at anywhere from $500 to $25,000 per meter diameter meter length. For the studies presented in this paper we used a value of $1,200/m^2, but additional studies have been performed using pipe costs of $5,000/m^2.

2.3 System Model Uses

The systems model is used in three principal ways. First, it can be used to identify the optimum operating conditions for particular components, such as the condenser or seawater predeaerator. The operating conditions identified in this study are being used to help define experimental conditions for future component tests at NELH. Secondly, the model provides information on the sensitivity of plant cost to various unknowns. These sensitivities can be used to rank research issues based on potential cost reductions. Even with uncertainty in the absolute cost predictions, relative differences are easily quantified. Finally, the model can be used (albeit cautiously) to predict costs and cost-effectiveness of open-cycle OTEC plants.

3.0 PASSIVE SEAWATER PREDEAERATION

3.1 Description

Natural seawater contains a small but significant amount of dissolved noncondensable gases, mainly nitrogen and oxygen [approximately 15 ppm total[23]]. These noncondensable gases come out of solution when the pressure is decreased on the fluid (for example in the evaporator or condenser). A significant parasitic power loss arises from the need to continuously exhaust noncondensable gases from the condenser to maintain the system vacuum. In addition, the presence of noncondensable gases degrades the condensation efficiency. It is possible to remove a portion of the dissolved gases without significant water vapor evolution by exposing the seawater to a pressure higher than the vapor pressure of the water before it enters the heat exchangers. Less power is then required because the desorbed gases are compressed and exhausted to the atmosphere from a pressure higher than the pressure in the condenser. A major factor influencing the desorption rate is the vapor-liquid interfacial area. Active methods for increasing this interfacial area, such as packed columns, have been examined in several studies,[3,14,22,28] but results indicate that the benefits of predeaeration are counteracted by the additional seawater pumping power required to provide the additional liquid head.

Recent results of experiments at NELH using natural seawater[18] indicate that these surface area promoting devices may not be required. A significant portion of the noncondensable gases was found to evolve in the supply upcomer for both warm and cold seawater. Figure 2 shows the fraction of equilibrium gas release for nitrogen and oxygen as a function of pressure in a debubbler chamber where the gas was vented to a compressor train. Fraction of equilibrium is defined as:

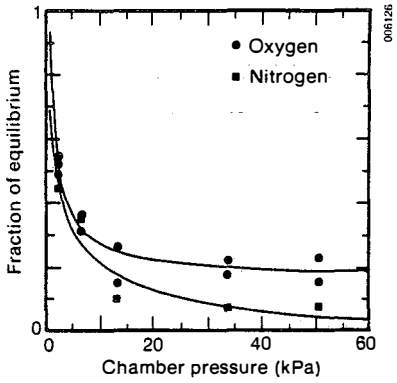

FIG. 2 HAWAII DEAERATION DATA: COLD SEAWATER

$$f_{eq} = (x_{in} - x_{out})/(x_{in} - x^*), \qquad (3)$$

where x_{in} is the inlet dissolved gas concentration, x_{out} is the measured outlet dissolved gas concentration, and x^* is the equilibrium outlet dissolved gas concentration defined by Henry's law:

$$x^* = He\ p_g \qquad (4)$$

He is Henry's constant for the gas and is a function of temperature, and p_g is the partial pressure of the gas above the liquid. The solid lines are data fit to curves used in the predeaeration subsystem model. The use of this data in the open-cycle systems model is preliminary since the mechanisms of gas release are not well understood at this time.

The fitted curves assume that gas release is a function only of chamber pressure. In fact, gas release is probably affected by the presence of nucleation sites, flow velocity, and pipe configuration. More extensive tests will be performed at the NELH including improved instrumentation such as in-line dissolved gas measurements. However, the present data are useful for examining the effects of passive predeaeration on system performance.

3.2 Seawater Predeaeration Subsystem Model

The noncondensable gas release curves shown in Fig. 3 were integrated into a seawater predeaeration subsystem model. A schematic of the model is shown in Fig. 4. The deaeration chambers and compressors for removing gases are staged. Referring to the diagram, the seawater first enters deaerator stage N, which is only slightly below atmospheric pressure. A portion of the noncondensable gases is released according to Eqs. 2 and 3. The seawater then progressively enters lower pressure chambers, releasing more gases. The seawater then enters the direct-contact heat exchangers. Because of the predeaeration, much less noncondensable gas is released in the main power cycle vacuum chambers. We assume the seawater head loss associated with each deaeration

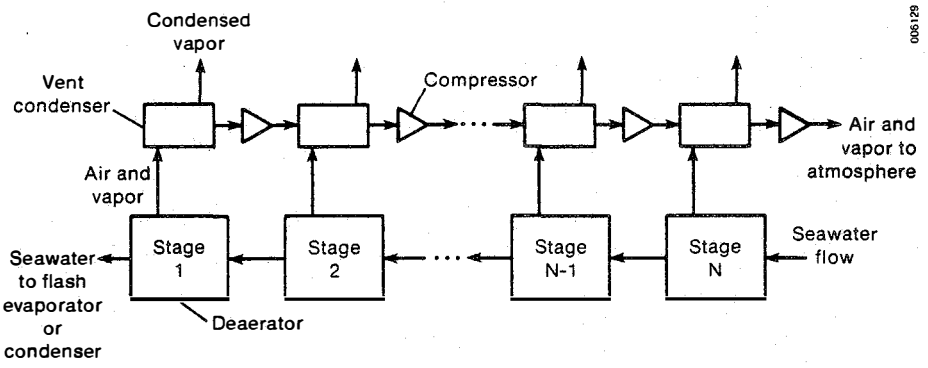

FIG. 3 DEAERATION SUBSYSTEM

stage to be negligible; therefore, we do not need to increase the seawater pumping power. Staging the deaerators maximizes gas release while minimizing the power requirements of the compressor. Interstage vent condenser and coolers are included to lower the temperature of the gas exiting a compressor and to reduce the water vapor flow rate in the next compressor. Compressor and intercooler cost equations are identical to those of the condenser exhaust system.[13] We assume the deaeration chamber cost to be negligible since it only consists of a small gas collection area in the seawater supply stream with a gas venting tap. In the predeaeration studies presented in this paper we used a structure cost of $\$25{,}000/m^2$ (as discussed in Sec. 2.2).

3.3 Predeaeration Assumptions and Results

System evaluations were made to quantify the effect of adding seawater predeaeration subsystems to the basic OC-OTEC plant. First, we optimized a plant without seawater predeaeration. Then, without changing the parameters that were varied to obtain the optimum plant, seawater predeaeration subsystems were added to both the warm and cold seawater flows. The number of compressor and deaerator stages was systematically increased to change the level of predeaeration. For this paper all the compressor pressure ratios were fixed at 1.6. Larger values of pressure ratio lead to increased parasitic power and would not allow us to examine many levels of deaeration. Smaller pressure ratios are not generally available for large volumetric flow rates and may lead to design problems and difficulty in estimating costs. The intercooler vapor pressure drop was set to 150 Pa, which corresponds to values from experimental and numerical studies for an efficient direct-contact device.[7,19] With this pressure drop and pressure ratio, the maximum number of stages on the warm side was 7 and on the cold side, 10. Additional stages lead to boiling in the lowest pressure deaerator.

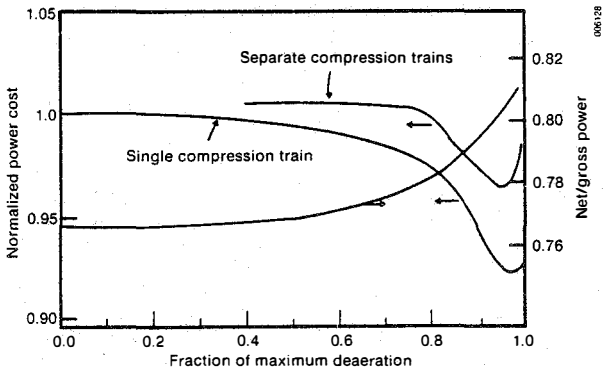

FIG. 4 EFFECTS OF DEAERATION ON SYSTEM PERFORMANCE AND COST

The reduction in normalized installed power cost in \$/watt and the increase in net/gross power ratio for various fractions of maximum deaeration, defined as

$$f_{md} = (P_{atm} - P_{min})/(P_{atm} - P_{sat}) , \qquad (5)$$

where P_{atm} is atmospheric pressure, P_{min} is the lowest deaerator stage pressure, and P_{sat} is the water vapor pressure, are shown in Fig. 4. Two cost curves are presented. One is for a single compression train where the vapor from each deaeration chamber is fed into the condenser exhaust compression train at the appropriate points. Another is for separate compression trains for the warm seawater predeaeration subsystem, the cold seawater predeaeration subsystem, and the condenser exhaust subsystem. Separate compression trains may allow for a greater degree of plant control, but costs are increased since the compressor cost versus volumetric flow relation does not have a zero intercept. The use of separate trains does not affect the net power of the plant since power is directly proportional to vapor flow. A maximum cost reduction of around 7%-8% is found at a fraction of maximum deaeration of 0.95. If the plant conditions were reoptimized or the pressure ratios were fine tuned by not assuming a constant value, a further reduction in cost would be realized. Larger fractions lead to increased installed power cost because adding another stage

Table 3. Effect of Evaporator Geometry on Installed Power Cost

Geometric Parameter	Nominal Value	Parametric Range	Resulting Normalized Cost Range
Spout height	0.5 m	0.2 - 2.0 m	0.98 - 1.05
Spout diameter	0.13 m	0.05 - 0.5 m	1.01 - 0.995
Spout seawater velocity (constant liquid loading)	2.0 m/s	0.5 - 4.0 m/s	0.98 1.04

does not significantly reduce the amount of noncondensable gases removed. Unlike previous studies[3,22] examining active deaeration schemes, this study indicates that including seawater predeaeration subsystems with passive deaerators is worthwhile in OC-OTEC plants because of the ease of gas desorption and the lack of any detrimental liquid head loss. Predeaeration subsystems were used in subsequent optimization studies.

4.0 EVAPORATOR PARAMETRIC STUDIES AND RESULTS

Parametric variations of vertical spout evaporator geometry and performance were completed so we could evaluate their effects on normalized installed power cost in $/watt. As mentioned earlier, no interactions between geometry and effectiveness are included in the model. Table 3 lists the nominal condition, parametric range, and effect on normalized installed power cost of several geometric parameters. The nominal plant in this case is an optimized 10-MW_e plant using the best seawater predeaeration subsystems defined in the study of Sec. 3.

Figure 5 shows the effect of varying the liquid loading and evaporator effectiveness, defined earlier, on normalized cost. Two sets of curves are presented. The first uses a vacuum structure cost of \$25,000/m^2. The effect of liquid loading and evaporator effectiveness on installed power cost is much more pronounced than the effects of

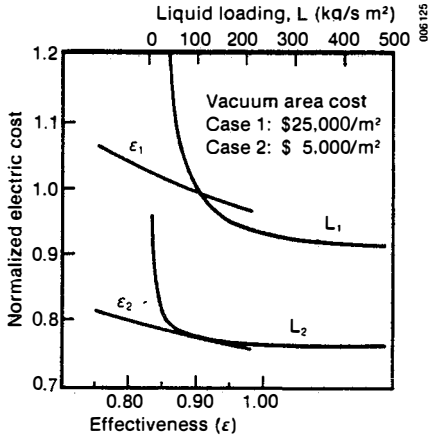

FIG. 5 EFFECTS OF EVAPORATOR PERFORMANCE AND LOADING ON POWER COST

the parameters presented in Table 3. Changing the vacuum area cost to \$5,000/m^2 significantly reduces the total cost and reduces the effects of these variables. In a practical system liquid loadings greater than 100-150 kg/s m^2 may lead to severe vapor escape problems.

These parametric studies are useful in defining the variables of importance in evaporator design. They suggest that further seawater experiments should concentrate on verifying the high-effectiveness values obtained in fresh water and the limited seawater tests and on examining the effect of increasing the liquid loading. The height of the spout required to maintain a high effectiveness is also of concern. Once interactions between spout geometry and performance are established, the results will be incorporated into the systems model for further optimization and study.

5.0 DIRECT-CONTACT CONDENSER STUDIES

5.1 Configuration and Model Basis

The condenser included in these studies is a two-stage, direct-contact device schematically shown in Fig. 6. Although surface condensers have also been studied for use in open-cycle OTEC, they are not discussed in this paper. A cocurrent followed by a countercurrent configuration is used. A cocurrent first stage is used for several reasons. In most open-cycle plant designs steam exits the turbine above the barometric level of the condenser either horizontally or vertically downward. By directing the steam downward the cost and pressure drop associated with a large steam passage to redirect the steam is avoided. In addition, the vapor side pressure drop (which is very important in low driving potential systems like OTEC) of a cocurrent section is low. After a large portion of the steam is condensed (70%-95%), the steam is turned upward and directed through a countercurrent section. Even though only a small portion of the steam is condensed in the countercurrent section, concentrating the noncondensable gases greatly reduces the exhaust pumping power.

The condenser model used in these studies is derived from results of detailed numerical codes[7,19] using the Colburn-Hougen[29] approach. Output was compared with results from freshwater condenser experiments with reasonable agreement. Because of the relatively large concentration of noncondensables in the steam, the detailed model evaluates local heat and mass transfer coefficients

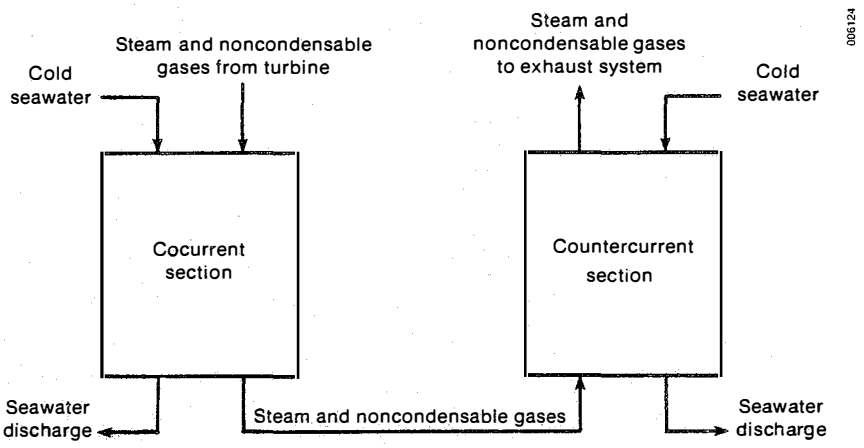

FIG. 6 TWO-STAGE, DIRECT-CONTACT CONDENSER

at discrete intervals. To keep computer costs at a reasonable level integrated results of the detailed numerical model were fit to curves with geometric and design variables as parameters in the systems code condenser subroutine.

5.2 Assumptions and System Results

The direct-contact condenser model used in the system studies has several inherent assumptions. The performance fitted curves assume a constant cross-sectional area and interfacial surface area per unit volume. It may be possible to improve performance by tailoring these parameters to best fit the local conditions at a given height in the condenser, but these second-order refinements are not yet included in the code. The code assumes a water distribution and drain collection height of 0.5 m. For conservative predictions condensation in these areas is not considered. In addition to the piping, floor, and vacuum structure costs discussed in Block et al.,[13] a $\$225/m^3$ charge for packing in the countercurrent section and $\$14/m^2$ for plate plus a water manifold charge for the falling film cocurrent section are included. Steam pressure losses past the water distribution manifold are assumed to be negligible.

Table 4. Comparison of System Operating Conditions for Two Vacuum Area Costs

	$\$5,000/m^2$	$\$25,000/m^2$
Cocurrent section		
Height (m)	1.75	2.00
Percentage condensed	91	87
Gas loading ($kg/s\ m^2$)	0.7	1.0
Outlet superheat (^oC)	0.8	2.1
Countercurrent section		
Height (m)	2.00	2.75
Percentage condensed	99	99
Gas loading ($kg/s\ m^2$)	0.4	0.5
Outlet superheat (^oC)	2.9	4.8

We optimized the condenser for the two vacuum area costs used in the evaporator studies. Table 4 compares the resulting condenser design parameters. At higher vacuum area cost the optimum vapor loading is increased in spite of higher pressure losses. In addition, contactor height is increased to make up for a slightly lower condensation efficiency. The increased outlet vapor superheat is a result of the larger pressure drop. We also studied the parameters of each design variable to examine the sensitivity of the optima. An example of this procedure is shown in Fig. 7 where normalized installed plant cost is plotted as a function of the cocurrent section height. The relatively low sensitivity of plant cost to cocurrent height allows a nominal height of 1.75 m to be selected for experiments even without certainty in the structure cost.

These results have been used to define reasonable ranges of design variables for condenser seawater tests. Verification of these performance predictions with seawater is critical. However, if the current model is accurate, condenser design parameters may vary over a fairly wide range without largely affecting installed power cost.

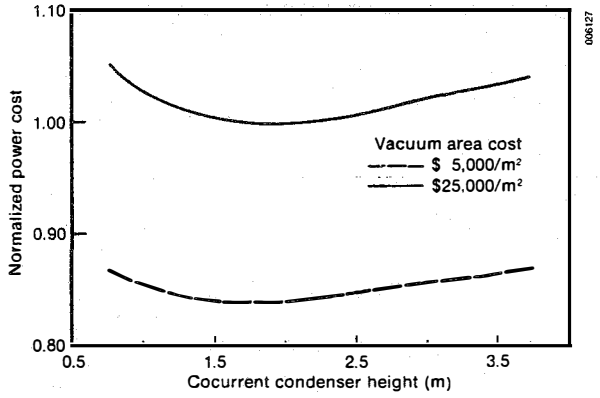

FIG. 7 EFFECTS OF VARYING THE COCURRENT HEIGHT ON POWER COST

6.0 CONCLUSIONS AND RECOMMENDATIONS

Using preliminary data on the performance of low-head deaerators quantifies the effect of using seawater predeaeration subsystems on open-cycle OTEC-installed power cost. Reductions in cost of 8% and an increase in the net/gross power ratio of 4% were demonstrated; further improvements are possible by fine tuning the predeaeration subsystem and reoptimizing the overall system. The cost difference between using a single compression train and separate compression trains for the warm predeaerators, cold predeaerators, and condenser exhaust was around 4%. It must be emphasized that the data must be verified and the mechanisms of gas release in these devices must be understood. This could lead to enhancing the performance and improved overall design.

Parametric studies that varied vertical spout evaporator geometry and performance indicate that the key parameters are maximum liquid loading and evaporator effectiveness. Experiments at NELH will concentrate on verifying model predictions and establish the needed relations between geometry and performance.

Using the systems model, optimum condenser operating conditions for two structure cost algorithms were identified. Large variations in parameters were not observed. These results have been used to define operating conditions for seawater experiments. Sensitivity of the plant cost to changes in condenser design conditions was generally less than 5%. Future efforts at SERI will include an expanded analytical effort to examine other direct-contact condenser geometries and the effects of transfer coefficient variations.

There is a critical need for seawater experiments to verify analytical model results, establish relations for interaction that are not addressed in the current models, and examine component coupling and integration effects. Planned future efforts include developing analytical models for additional condenser geometries and component seawater experiments at NELH.

7.0 ACKNOWLEDGMENT

We wish to acknowledge and express our gratitude to DOE's Ocean Energy Program, which sponsored this research and to the researchers at NELH for use of their data in the deaeration model.

8.0 REFERENCES

1. D'Arsonval, Arsene, "Utilisation des forces natuelles: Avenir de L'electricite," La Revue Scientifique, 17 Sept 1881, pp. 370-372.

2. Claude, Georges, "Power from the Tropical Seas," Mechanical Engineering, Vol. 52, No. 12, December 1930, pp. 1039-1044.

3. Westinghouse Electric Corporation, 100 MW_e OTEC Alternate Power Systems, U.S. DOE Contract No. EG-77-C-05-1473, Vol. 1, March 1979.

4. Bharathan, D., Kreith, F., and Owens, W. L., "An Overview of Heat and Mass Transfer in Open-Cycle OTEC Systems," ASME/JSME Thermal Engineering Joint Conference Proceedings, Y. Mori and W. J. Wang, eds., Vol. 2, pp. 301-314, 1983.

5. Bharathan, D., and Penney, T., "Flash Evaporation from Falling Turbulent Jets," ASME/JSME Thermal Engineering Joint Conference Proceedings, Y. Mori and W. J. Wang, eds., Vol. 2, pp. 341-353, 1983.

6. Bharathan, D., and Penney, T., Mist Eliminators for Freshwater Production from Open-Cycle OTEC Systems, SERI/TR-252-1991, Golden, CO: Solar Energy Research Institute, December 1983.

7. Wassel, A. T., Bugby, D. C., Mills, A. F., and Farr, J. L., Jr., "Design Methodology for Direct-Contact Falling Film Evaporators and Condensers for Open-Cycle Ocean Thermal Energy Conversion," SAI-083-83R-001, El Segundo, CA: Science Applications Inc., February 1982.

8. Bharathan, D., Olson, D. A., Green, H. J., and Johnson, D. M., "Measured Performance of Direct-Contact Jet Condensers," SERI/TP-252-1437, Golden, CO: Solar Energy Research Institute, January 1982.

9. Sam, R. G., and Patel, B. R., "Open-Cycle Ocean Thermal Energy Conversion Evaporator/Condenser Test Program--Data Report," TN-340, Hanover, NH: Creare Research and Development, Inc., October 1982.

10. Parsons, B.P., Bharathan, D., and Althof, J.A., Thermodynamic Systems Analysis of Open-Cycle Ocean Thermal Energy Conversion, SERI/TR-252-2234, Golden, CO: Solar Energy Research Institute.

11. Penney, T., Bharathan, D., Althof, J., and Parsons, B., "Small-Scale, Shore-Based, Open-Cycle Ocean Thermal Energy Conversion Systems--A Design Case Study for an Integrated Research Facility," SERI/TP-252-2331, Golden, CO: Solar Energy Research Institute, forthcoming.

12. Bharathan, D., and Althof, J., "An Experimental Study of Steam Condensation on Water in Countercurrent Flow in Presence of Inert Gases," SERI/TP-252-2332, Golden, CO: Solar Energy Research Institute.

13. Block, David L., et al., Thermoeconomic Optimization of OC-OTEC Electricity and Water Plants, SERI Contract No. XX-3-03077-1, Final Report, September 1984.

14. Parsons, B.K., Althof, J.A., and Bharathan, D., "Open-Cycle OTEC Thermal-Hydraulic Systems Analysis and Parametric Studies," Oceans '84, September 1984.

15. Penney, T., et al., "Open-Cycle Ocean Thermal Energy Conversion (OTEC) Research: Progress Summary and a Design Study," ASME 84-WA/SOL 26, December 1984.

16. Valenzuela, J. A., et al., "Thermoeconomic Analysis of Open-Cycle OTEC Plants," Creare R&D Inc., ASME 84-WA/SOL-24, December 1984.

17. Krock, H. J., and Zapka, M. J., "Open-Cycle OTEC Non-Condensable Gas Exchange Characteristics," Intersol '85, International Solar Energy Society Conference, Montreal, Canada, June 1985.

18. Penney, T. R., and Althof, J. A., "Measurements of Gas Sorption from Seawater and the Influence of Gas Release on Open-Cycle Ocean Thermal Energy Conversion (OC-OTEC) System Performance," Intersol '85, International Solar Energy Society Conference, Montreal, Canada, June 1985.

19. Bharathon, D., Althof, J., and Parsons, B., Direct-Contact Condensers for Open-Cycle Ocean Thermal Energy Conversion (OTEC) Applications, Draft Report RR-252-2472, Golden, CO: Solar Energy Research Institute, 1985.

20. Larson-Basse, J., Open-Cycle Ocean Thermal Energy Conversion Experiment, Preliminary Report to the Solar Energy Research Institute, Golden, Colorado, 1983.

21. Wassel, A. T., Bugby, D. C., and Mills, A. F., Bubble Nucleation and Growth in Open-Cycle Ocean Thermal Energy Conversion Subsystems, SAI-083-83R-002, Science Applications Inc., 1982.

22. Golshani, A., and Chen, F. C., Ocean Thermal Energy Conversion Gas Desorption Studies, ORNL/Tm-7438/V, Oak Ridge National Laboratory, Oak Ridge, TN, 1981.

23. Krock, H. J., Gas Analysis of Water Samples for OTEC Program, Technical Report No. 51, J. K. K. Look Laboratory, University of Hawaii, Honolulu, 1981.

24. Jennings, S. J., "Ocean Thermal Energy Conversion," Open-Cycle Ocean Thermal Energy Conversion Low-Pressure Turbine Development Program, Dynamic and Off Design Analysis, Interim Report No. 6, Westinghouse Electric Corp., June 1982.

25. Penney, T., unpublished Letter Report from A. T. Wassel, Hermosa Beach, CA: Science Applications, Inc., 14 July 1983.

26. Shelpuk, B. C., "A 165-kW Open-Cycle OTEC Experiment," presented at the 12th Annual Intersociety Energy Conversion Engineering Conference 1985, Miami Beach, FL, 18-23 August 1985.

27. Research and Development, October 1984, Barrington, IL.

28. Marchand, P., "Recent French OTEC Work in the Area of OTEC Systems," 7th Ocean Energy Conference, Washington, D.C., June 1980.

29. Colburn, A. P., and Hougen, O. A., "Design of Cooler Condensers for Mixtures of Vapors with Noncondensing Gases," Industrial and Engineering Chemistry, Vol. 26, pp. 1178-1182, November 1934.